THE JOURNAL OF BIOLOGICAL CHEMISTRY
Vol. 273, No. 21, Issue of May 22, pp. 13182–13188, 1998

Printed in U.S.A.

Substrate Specificity of δ Ribozyme Cleavage*

(Received for publication, October 30, 1997, and in revised form, January 26, 1998)

Sirinart Ananvoranich‡ and Jean-Pierre Perreault§

From the Département de biochimie, Faculté de médecine, Université de Sherbrooke, Québec, J1H 5N4, Canada

The specificity of δ ribozyme cleavage was investigated using a *trans*-acting antigenomic δ ribozyme. Under single turnover conditions, the wild type ribozyme cleaved the 11-mer ribonucleotide substrate with a rate constant of 0.34 min^{-1}, an apparent K_m of 17.9 nM and an apparent second-order rate constant of 1.89×10^7 min^{-1} M^{-1}. The substrate specificity of the δ ribozyme was thoroughly investigated using a collection of substrates that varied in either the length or the nucleotide sequence of their P1 stems. We observed that not only is the base pairing of the substrate and the ribozyme important to cleavage activity, but also both the identity and the combination of the nucleotide sequence in the substrates are essential for cleavage activity. We show that the nucleotides in the middle of the P1 stem are essential for substrate binding and subsequent steps in the cleavage pathway. The introduction of any mismatches at these positions resulted in a complete lack of cleavage by the wild type ribozyme. Our findings suggest that factors more complex than simple base pairing interactions, such as tertiary structure interactions, could play an important role in the substrate specificity of δ ribozyme cleavage.

δ ribozymes derived from the genome of hepatitis δ virus (HDV)[1] are metalloenzymes. Like other catalytically active ribozymes, namely hammerhead and hairpin ribozymes, the δ ribozymes cleave a phosphodiester bond of their RNA substrates and give rise to reaction products containing a 5′-hydroxyl and a 2′,3′-cyclic phosphate termini. Two forms of δ ribozymes, namely genomic and antigenomic, were derived and referred to by the polarity of the HDV genome from which the ribozyme was generated. Both δ ribozyme forms exhibit self-cleavage activity, and it has been suggested that they are involved in the process of viral replication (1). This type of activity has been described as *cis*-acting δ ribozymes (2).

Like other ribozymes, δ ribozymes have a potential application in gene therapy in which an engineered ribozyme is directed to inhibit gene expression by targeting a specific mRNA molecule. It has been demonstrated that a very low concentration (<0.1 mM) of Ca^{2+} and Mg^{2+} is required for δ ribozyme cleavage (3). δ ribozymes have a unique characteristic in their substrate binding, namely that only the 3′-portion of the substrate is required for binding to the ribozyme. A short stretch of nucleotides (7 nt) located on the substrate is required for cleavage. Although one might suspect the specificity of δ ribozyme cleavages due to their short recognition site, we view this characteristic of the δ ribozyme as an advantage for the future development of a therapeutic means of controlling, for example, a viral infection.

Since little is known about the kinetic properties of δ ribozymes, study of the *trans*-acting system will enable us to answer some basic questions on both the structure required and the kinetic properties, including the substrate specificity, of δ ribozymes. Depending on the predicted secondary structures used, various *trans*-acting δ ribozyme systems were generated by separating the RNA molecule into ribozyme and substrate molecules at various positions (4–6). Here, we generate a *trans*-acting δ ribozyme, based on the pseudo knot-like structure proposed by Perrotta and Been (2), by separating the single-stranded region located at the junction between the P1 and P2 stems (Fig. 1). Although, several investigations have been performed to address the questions related to the substrate specificity of δ ribozymes in both the *cis*- and *trans*-acting forms (2, 5–12), most, if not all, experiments were carried out by randomly changing the base pairing combinations or by introducing mismatches which interfere with the Watson-Crick base pairing between the substrate and the ribozyme in the P1 stem (Fig. 1). It was demonstrated that cleavage activity was not destroyed by the interchanging of one to four nucleotide pairs between the substrate and the δ ribozyme (2, 8, 11, 12). One or two nucleotide mismatches at any position of the P1 stem, except positions 5 and 11 (numbering according to Fig. 1), completely destroyed the activity (2, 5–12). Although these are composite results from various versions of δ ribozymes, these findings could be interpreted as indicating that the positions located at both extremities of the base paired stem formed by the substrate and the ribozyme were more likely to tolerate a mismatch, resulting in distortion of the P1 stem, than the internal positions. There is no information on how each nucleotide of the substrate affects the cleavage activity and its kinetics since most investigations were carried out at only one or two positions at a time, and the findings generally reported in a plus/minus manner (*e.g.* cut or uncut). Therefore, the substrate specificity of δ ribozyme could not be deduced from previous reports. To determine how substrate sequences affect δ ribozyme cleavage activity, we performed kinetic studies using a collection of short oligonucleotide substrates (11 nt) with a *trans*-acting δ ribozyme. In this report, we demonstrate that each nucleotide of the P1 stem contributes differently to the cleavage activity. We compare the observed cleavage rate constants for cleavable substrates and the equilibrium dissociation constants for the uncleavable substrates with those of the wild type substrate. We present evidence that strongly suggests that the nucleotides located in the center of the P1 stem formed between substrate and ribozyme (Fig. 1, positions 7 and 8) are important not only for substrate recognition but probably also for subsequent steps, for example a conformation change yielding a transition complex.

* This work was supported in part by a grant from the Medical Research Council (MRC) of Canada (to J. P. P.). The costs of publication of this article were defrayed in part by the payment of page charges. This article must therefore be hereby marked "*advertisement*" in accordance with 18 U.S.C. Section 1734 solely to indicate this fact.

‡ Recipient of a postdoctoral fellowship from Natural Sciences and Engineering Research Council (NSERC) of Canada.

§ Medical Research Council scholar. To whom correspondence should be addressed. Tel.: 819-564-5310; Fax: 819-564-5340; E-mail: jp.perre@courrier.usherb.ca.

[1] The abbreviations used are: HDV, hepatitis δ virus; nt, nucleotide(s).

MATERIALS AND METHODS

Plasmids Carrying δ Ribozymes

The antigenomic ribozyme sequence of the hepatitis δ virus described by Makino *et al.* (13) was used to generate a *trans*-acting δ ribozyme with some modifications as shown in Fig. 1. Briefly, the construction was performed as follows. Two pairs of complementary and overlapping oligonucleotides, representing the entire length of the ribozyme (57 nt), were synthesized and subjected to an annealing process prior to cloning into pUC19. The annealed oligonucleotides were ligated to *Hin*dIII and *Sma*I co-digested pUC19 to give rise to a plasmid harboring the δ ribozyme (referred to as pδRzP1.1). A mutant ribozyme (δRzP1.2) was then constructed by modifying the substrate recognition site of pδRzP1.1 by ligation of an oligonucleotide containing the altered sequence flanked by restriction endonuclease sites to *Rsr*II/*Sph*I predigested pδRzP1.1. The sequences of engineered ribozymes were confirmed by DNA sequencing. Plasmids containing wild type and mutant ribozymes were then prepared using Qiagen tip-100 (Qiagen Inc.), digested with *Sma*I, purified by phenol and chloroform extraction, and precipitated for further use as templates for *in vitro* transcription reactions.

RNA Synthesis

Ribozyme—In vitro transcription reactions contained 5 μg of linearized recombinant plasmid DNA as template, 27 units RNAGuard® RNase inhibitor (Amersham Pharmacia Biotech), 4 mM of each ribonucleotide (Amersham Pharmacia Biotech), 80 mM HEPES-KOH, pH 7.5, 24 mM $MgCl_2$, 2 mM spermidine, 40 mM dithiothreitol, 0.01 unit of pyrophosphatase (Boehringer Mannheim) and 25 μg of purified T7 RNA polymerase in a final volume of 50 μl, and were incubated at 37 °C for 4 h.

Substrates—Deoxyoligonucleotides (500 pmol) containing the substrate and T7 promoter sequence were denatured by heating at 95 °C for 5 min in a 20-μl mixture containing 10 mM Tris-HCl, pH 7.5, 10 mM $MgCl_2$, 50 mM KCl_2, and allowed to cool slowly to 37 °C. The *in vitro* transcription reactions were carried out using the resulting partial duplex formed as template under the same conditions as described for the production of the ribozyme.

After incubation, the reaction mixtures were fractionated by denaturing 20% polyacrylamide gel electrophoresis (19:1 ratio of acrylamide to bisacrylamide) containing 45 mM Tris borate, pH 7.5, 7 M urea, and 1 mM EDTA. The reaction products were visualized by UV shadowing. The bands corresponding to the correct sizes of either ribozymes or substrates were cut out, and the transcripts eluted overnight at 4 °C in a solution containing 0.1% SDS and 0.5 M ammonium acetate. The transcripts were then precipitated by the addition of 0.1 volume of 3 M sodium acetate, pH 5.2, and 2.2 volumes of ethanol. Transcript yield was determined by spectrophotometry.

End-labeling of RNA with [γ-^{32}P]ATP

Purified transcripts (10 pmol) were dephosphorylated in a 20-μl reaction mixture containing 200 mM Tris-HCl, pH 8.0, 10 units of RNAGuard®, and 0.2 units of calf intestine alkaline phosphatase (Amersham Pharmacia Biotech). The mixture was incubated at 37 °C for 30 min and then extracted twice with a same volume of phenol:chloroform (1:1). Dephosphorylated transcripts (1 pmol) were end-labeled in a mixture containing 1.6 pmol [γ-^{32}P]ATP, 10 mM, Tris-HCl, pH 7.5, 10 mM $MgCl_2$, 50 mM KCl, and 3 units of T4 polynucleotide kinase (Amersham Pharmacia Biotech) at 37 °C for 30 min. Excess [γ-^{32}P]ATP was removed by applying the reaction mixture onto a spin column packed with a G-50 Sephadex gel matrix (Amersham Pharmacia Biotech). The concentration of labeled transcripts was adjusted to 0.01 pmol/ml by the addition of water.

Cleavage Reactions

To initiate a cleavage reaction, we tested different procedures and chose the method that yielded the highest cleavage rate constant and the maximum cleavage product as described by Fauzi *et al.* (14). Various concentrations of ribozymes were mixed with trace amounts of substrate (final concentration <1 nM) in a 18-μl reaction mixture containing 50 mM Tris-HCl, pH 7.5, and subjected to denaturation by heating at 95 °C for 2 min. The mixtures were quickly placed on ice for 2 min and equilibrated to 37 °C for 5 min prior to the initiation of the reaction. Unless stated otherwise, cleavage was initiated by the addition of $MgCl_2$ to 10 mM final concentration. The cleavage reactions were incubated at 37 °C, and followed for 3.5 h or until the end point of cleavage was reached. The reaction mixtures were periodically sampled (2–3 μl), and these samples were quenched by the addition of 5 μl of stop solution containing 95% formamide, 10 mM EDTA, 0.05% bromphenol blue, and 0.05% xylene cyanol. The resulting samples were analyzed by a 20% polyacrylamide gel electrophoresis as described above. Both the substrate (11 nt) and the reaction product (4 nt) bands were detected using a Molecular Dynamics radioanalytic scanner after exposition of the gels to a phosphorimaging screen.

Kinetic Analysis

Measurement of Pseudo First-order Rate Constant (k_{cat}, K_m and k_{cat}/K_m)—Kinetic analyses were performed under single turnover conditions as described by Hertel *et al.* (15) with some modifications. Briefly, trace amounts of end-labeled substrate (<1 nM) were cleaved by various ribozyme concentrations (5–500 nM). The fraction cleaved was determined, and the rate of cleavage (k_{obs}) obtained from fitting the data to the equation $A_t = A_\infty(1 - e^{-kt})$ where A_t is the percentage of cleavage at time t, A_∞ is the maximum percent cleavage (or the end point of cleavage), and k is the rate constant (k_{obs}). Each rate constant was calculated from at least two measurements. The values of k_{obs} obtained were then plotted as a function of ribozyme concentrations for determination of the other kinetic parameters: k_{cat}, K_m and k_{cat}/K_m. Values obtained from independent experiments varied less than 15%. The requirement for Mg^{2+} by both ribozymes was studied by incubating the reaction mixtures with various concentrations of $MgCl_2$ (1–500 mM) in the presence of an excess of ribozyme (500 nM) over substrate (<1 nM). The concentrations of Mg^{2+} at the half-maximal velocity were determined for both ribozymes.

Determination of Equilibrium Dissociation Constants (K_d)—For mismatched substrates that could not be cleaved by the ribozyme, the equilibrium dissociation constants were determined using a slight modification of the method described by Fedor and Uhlenbeck (16). Eleven different ribozyme concentrations, ranging from 5 to 600 nM, were individually mixed with trace amounts of end-labeled substrates (<1 nM) in a 9-μl solution containing 50 mM Tris-HCl, pH 7.5, heated at 95 °C for 2 min and cooled to 37 °C for 5 min prior to the addition of $MgCl_2$ to a final concentration of 10 mM, in a manner similar to that of a regular cleavage reaction. The samples were incubated at 37 °C for 1.5 h, at which time 2 μl of sample loading solution (50% glycerol, 0.025% of each bromphenol blue and xylene cyanol) was added, and the resulting mixtures were electrophoresed through a nondenaturing polyacrylamide gel (20% acrylamide with a 19:1 ratio of acrylamide to bisacrylamide, 45 mM Tris borate buffer, pH 7.5 and 10 mM $MgCl_2$). Polyacrylamide gels were prerun at 20 W for 1 h prior to sample loading, and the migration was carried out at 15 W for 4.5 h at room temperature. Quantification of bound and free substrates was performed following an exposure of the gels to a phosphorimaging screen as described earlier.

RESULTS

The *trans*-acting δ ribozymes used in this report were derived from the antigenomic δ ribozyme of HDV (13). Some features of the antigenomic δ ribozyme were modified to improve its structural stability and to aid in transcript production. Based on a pseudo knot-like structure described by Perrotta and Been (2), Fig. 1 shows the structure of the δ ribozymes used with some modifications: (i) the single-stranded region between substrate and ribozyme (region J1/2) was eliminated to separate the substrate molecule from the ribozyme; (ii) the substrate contains only 11 nt and produces 7- and 4-nt cleavage products, and the GGG at the 5′-end was added to increase the yield during *in vitro* transcription (17); (iii) three G-C base pairs were introduced in the P2 region to improve both the structural stability and transcript production; and (iv) the P4 stem was shortened to the minimum length reported to result in an active ribozyme (18). Prior to performing a cleavage reaction, native gel electrophoresis was used to test for the possible presence of aggregates or multimer forms of the transcripts. Various concentrations of ribozyme, ranging from 5 nM to 2 μM, were mixed with trace amounts of end-labeled ribozyme (less than 0.5 nM) and fractionated under nondenaturing conditions as described under "Materials and Methods." We detected the presence of a slow migrating species of ribozyme in the mixture containing 2 μM ribozyme (data not shown). The quantification of the slow migrating band showed

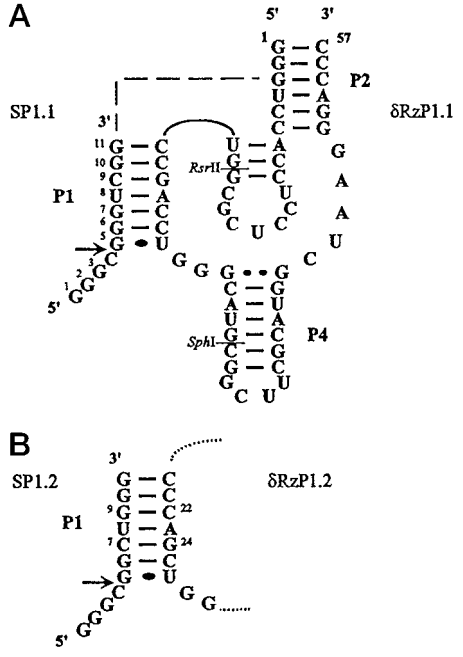

FIG. 1. **Secondary structure and nucleotide sequences of the constructed *trans*-acting antigenomic δ ribozymes and their complementary substrates.** The base paired regions of the pseudo knot-like structure are numbered according to Perrotta and Been (2). *Panel A*, secondary structure of the complex formed between δRzP1.1 and its substrate, SP1.1. The *arrow* indicates the cleavage site. The nucleotide numbering of the substrate is indicated and referred to throughout the text. The *dotted line* represents a single-strand region joining the substrate and ribozyme molecules as presented in the *cis*-form (namely J1/2, 2). This single-strand area was eliminated to produce the *trans*-acting ribozymes used in this study. *Panel B*, the P1 region of δRzP1.2 and its substrate, SP1.2. Two base pairs at positions 7 and 9 of the substrate and positions 22 and 24 of δRzP1.1 were swapped. δRzP1.2 was constructed using the *Rsr*II and *Sph*I restriction sites indicated on the structure of δRzP1.1 as described under "Materials and Methods." The rest of the structure is identical to δRzP1.1 as in *panel A*.

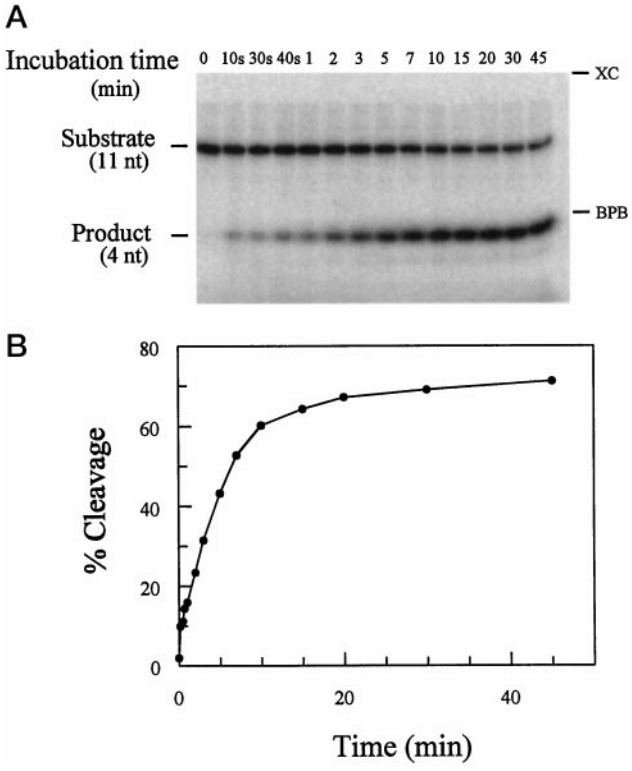

FIG. 2. **Time course for a cleavage reaction catalyzed by δRzP1.1.** *Panel A*, an autoradiogram of a polyacrylamide gel showing a cleavage assay carried out under single turnover conditions as described under "Materials and Methods." 100 nM δRzP1.1 were incubated with 1 nM end-labeled SP1.1 at 37 °C in the presence of 50 mM Tris-HCl, pH 7.5, and 10 mM $MgCl_2$. The positions of xylene cyanol (*XC*) and bromphenol blue (*BPB*) are indicated. *Panel B*, quantification of the data in *panel A*. A single exponential equation was used to fit data to k_{obs} = 0.21 min^{-1} and 68% as the extent of cleavage.

that the band amounted to approximately 2% of the total radioactive material. However, a single band was detected at the concentrations used for kinetic analysis and under single turnover conditions (5–600 nM). Similar experiments were performed for each substrate. There was no substrate multimer detected at the concentrations used (data not shown). The equimolar mixture of end-labeled substrate and ribozyme was also fractionated under nondenaturing conditions, and it resulted a single band of ribozyme and substrate complex similar to those observed for the K_d measurement shown in Fig. 4.

Cleavage Kinetics of Constructed Antigenomic δ Ribozymes

Two forms of *trans*-acting δ ribozymes (δRzP1.1 and δRzP1.2) were used with their corresponding substrates (11 nt) for the kinetic studies. δRzP1.2 differs from δRzP1.1 in that δRzP1.2 has two nucleotides, at positions 22 and 24 of δRzP1.1, interchanged (Fig. 1, 5′-CCCAGCU-3′). Time course experiments for cleavage reactions catalyzed by both δRzP1.1 and δRzP1.2 were monitored by the appearance of the 4 nt cleavage product. An example of a time course experiment for a cleavage reaction catalyzed by δRzP1.1 is shown in Fig. 2, *panel A*. In this particular experiment, 100 nM of δRzP1.1 was incubated with 1 nM end-labeled substrate, SP1.1. The newly formed product and the remaining substrate bands at each time point were quantified, and the percentage of cleavage was plotted as a function of time (Fig. 2, *panel B*). δRzP1.1 cleaved approximately 60% of the substrate within 10 min. The data were fitted to a single exponential equation as described under "Materials and Methods" so as to obtain the observed rate constant (k_{obs} = 0.21 min^{-1}). We attempted to fit the data as biphasic reactions as described for the hairpin (19) and the hammerhead (20) ribozymes. We observed that the standard deviation (χ^2) of data fitted to a double-exponential equation was higher (χ^2 = 0.01203) than that fitted to a single exponential equation (χ^2 = 0.000203). Although we could not exclude or dismiss completely the possibility that more than one conformation of the active ribozyme could be formed, the data were treated as if the reactions were monophasic in their kinetics for comparison purposes.

Similar experiments were performed using trace amounts of substrate (<1 nM) and various ribozyme concentrations to measure k_{obs} at each ribozyme concentration. The values of k_{obs} of both δRzP1.1 and δRzP1.2 increased with an increase in ribozyme concentration up to approximately 200 nM (Fig. 3, *panel A*). The concentration of ribozyme at which the reaction velocity reached half-maximal (apparent K_m, K_m') is 17.9 ± 5.6 nM for δRzP1.1 and 16.7 ± 6.4 nM for δRzP1.2. Under the reaction conditions used, in which the increase in ribozyme concentration has no significant effect on the rate of cleavage, the cleavage rate (k_{obs}) is therefore represented by the catalytic rate constant (k_{cat}). The cleavage rate constants are 0.34 min^{-1} for δRzP1.1 and 0.13 min^{-1} for δRzP1.2. Apparent second-order rate constants (k_{cat}/K_m') were calculated to be 1.89×10^7 min^{-1} M^{-1} for δRzP1.1 and 0.81×10^7 min^{-1} M^{-1} for δRzP1.2 (Table I).

Since we observed that the k_{cat} of δRzP1.2 is about 3 times less than that of δRzP1.1, whereas the K_m' is similar, we

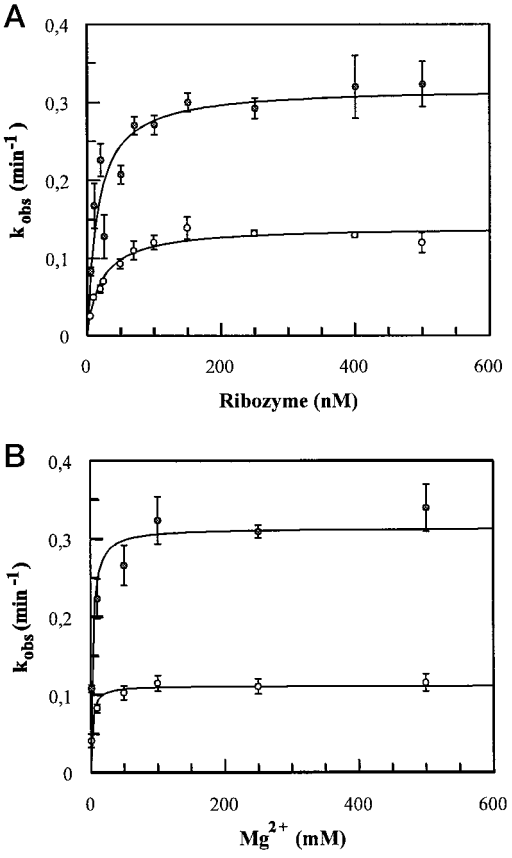

FIG. 3. **Kinetics of cleavage reactions catalyzed by *trans*-acting δ ribozymes.** *Panel A*, the observed cleavage rate constants were plotted as a function of ribozyme concentrations. The values of δRzP1.1 are indicate by ●; and those of δRzP1.2 by ○. The concentrations of ribozyme at half-velocity are 17.9 ± 5.6 nM for δRzP1.1 and 16.7 ± 6.4 nM for δRzP1.2. The values of k_{cat} is 0.34 min^{-1} for δRzP1.1 and 0.13 min^{-1} for δRzP1.2. Standard error from two independent experiments was less than 15%. *panel B*. The requirement of Mg^{2+} for cleavage reactions catalyzed by δRzP1.1 and δRzP1.2. Under single turnover conditions, 500 nM ribozymes were incubated with 1 nM end-labeled complementary substrates in the presence of various concentration of Mg^{2+}. The obtained initial cleavage rates were plotted as a function of the Mg^{2+} concentrations. The values of δRzP1.1 are indicated by ● and those of δRzP1.2 by ○. At 10 mM Mg^{2+}, which was used in a regular cleavage reaction, both ribozymes cleaved their substrates at their maximum rate (0.3 min^{-1} for δRzP1.1 and 0.1 min^{-1} for δRzP1.2).

TABLE I
Kinetic parameters of wild type ribozyme (δRzP1.1) and mutant ribozyme (δRzP1.2)

Under single turnover conditions, trace amounts of end-labeled substrate (<1 nM) were cleaved by various concentrations of ribozyme (5–600 nM). Reactions carried out under these conditions displayed monophasic kinetics. The values were calculated from at least two independent experiments, and standard variations were less than 15%.

Kinetic parameters	δRzP1.1	δRzP1.2
k_{cat} (min^{-1})	0.34 ± 0.02	0.13 ± 0.01
K_m' (nM)	17.9 ± 5.6	16.7 ± 6.4
k_{cat}/K_m' (min^{-1} M^{-1})	1.89×10^7	0.81×10^7
K_{Mg} (mM)	2.2 ± 1.0	2.1 ± 0.8

investigated whether an increased amount of Mg^{2+} in the cleavage reaction would affect the k_{cat} of δRzP1.2. Under single turnover conditions, in which the ribozyme and substrate concentrations were kept at 500 and 1 nm, respectively, we found that both ribozymes cleave their complementary substrates at Mg^{2+} concentrations as low as 1 mM, which is the estimated physiological concentration of Mg^{2+} (21). At this concentration, the k_{obs} obtained were 0.11 ± 0.01 and 0.04 ± 0.01 min^{-1}, for δRzP1.1 and δRzP1.2, respectively (Fig. 3, *panel B*). A maximum k_{obs} for δRzP1.2 was observed when the concentration of Mg^{2+} was 10 mM. Higher concentrations of Mg^{2+} did not increase either the k_{obs} or the extent of cleavage for both ribozymes. We did not observe a decrease in the cleavage rate when higher concentrations of Mg^{2+} were used (*e.g.* 500 mM). The requirement for magnesium at half-maximal velocity (K_{Mg}) was 2 mM for both δRzP1.1 and δRzP1.2.

Substrate Specificity

To compare the specificity of the δ ribozyme with various substrates, δRzP1.1 was used under single turnover conditions as described above. The cleavage reactions were performed with a trace amount of each substrate (<1 nM) and 500 nM δRzP1.1. Under these conditions, the observed rates reflect the rates of cleavage without interference from either product dissociation or inhibition. For each substrate both the observed cleavage rate constants (k_{obs}) and the extent of cleavage were calculated and compared with those of the wild type substrate, as shown in Table II.

Shorter Substrates—Three shorter substrates containing 10, 9, and 8 nt were tested individually and compared with the 11-nt substrate (SP1.1) in which 7 nt base paired with δRzP1.1. The 10-, 9-, and 8-nt substrates contain 6, 5, and 4 nt regions complementary to δRzP1.1, respectively. We observed that the 10-nt substrate was cleaved with a k_{obs} of 0.02 ± 0.01 min^{-1} and a maximal cleavage of 28.8% (Table II). We could not detect the cleavage product formed when the 9- and 8-nt substrates were used, even after a 3.5-h incubation time. The cleavage reactions were also carried out in the presence of 100 mM Mg^{2+} instead of the 10 mM concentration used in a regular cleavage reaction. We observed no improvement in the values of the k_{obs} and the extent of cleavage for the 10-nt substrate and still detected no cleavage for both the 9- and 8-nt substrates.

Mismatched Substrates—We have generated a collection of substrates in which single mismatches were individually introduced into the P1 region of the substrate and then used in the cleavage reactions (Table II). Mutation at position 5 resulted in at least a 9-fold decrease in k_{obs} as compared with that of SP1.1 (0.34 min^{-1}). However, for SG5A, in which A was substituted for G at position 5 of SP1.1, the extent of cleavage was only reduced by half. When this nucleotide was changed to cytosine, the cleavage was reduced almost to nil (*ca.* 1.7%). δRzP1.1 cleaved approximately 4% of the SG6A and SG6U substrates, in which A or U were substituted for G at position 6. The alteration of either position 7 or 8, located in the middle of the P1 stem, yielded uncleavable substrates (SG7A, SG7U, SU8C, SU8G). The k_{obs} was also drastically decreased when the C at position 9 was altered to A or U. The extent of cleavage was reduced to approximately 50%, when SC9U was used. The SG10U substrate, in which U was substituted for G at position 10, gave a similar result to SC9A. Finally, δRzP1.1 cleaved the substrate SG11U almost as well as SP1.1, although the k_{obs} was considerably slower (0.01 min^{-1}). The relative activity of each single mismatched substrate was calculated to obtain an apparent free energy of transition-state stabilization, $\Delta\Delta G^{\ddagger}$ (22, 23). We found that the values of $\Delta\Delta G^{\ddagger}$ range between −0.96 to −2.25 kcal^{-1} mol^{-1}. This apparent difference in activation energy was also observed when substrates of leadzyme were altered and used in a cleavage assay (22).

Equilibrium Dissociation Constant (K_d)

The four substrates containing a single mismatch either at position 7 or 8, which were not cleaved by δRzP1.1, were used to determine an equilibrium dissociation constant (K_d). Trace amounts of end-labeled substrates (SG7A, SG7U, SU8C, or SU8G) were individually incubated with various concentra-

TABLE II

Cleavage activity of shorter or mismatched substrates as compared to the wild type substrate (SP1.1)

Bold letters represent the nucleotides of wild type substrate recognized by δRzP1.1. The numbers in subscript indicate the nucleotides of wild type substrate that were individually altered to generate shorter or mismatched substrates. k_{obs} is the observed rate of cleavage calculated from at least two measurements. Cleavage extent (%) is obtained by fitting the data to the equation $A_t = A_\infty (1 - e^{-kt})$, where A_t is the percentage of cleavage at time t, A_∞ is the maximum percentage of cleavage, and k is the rate constant. k_{rel} is the relative rate constant as compared to that of wild-type substrate. $\Delta\Delta G^\ddagger$, the apparent free energy of transition-state stabilization, was calculated using the equation $\Delta\Delta G^\ddagger = RT \ln k_{rel}$, where $T = 310.15$ K (37 °C) and $R = 1.987$ cal · $K^{-1}mol^{-1}$.

Substrates	Sequence	k_{obs}	Extent of cleavage	k_{rel}	$\Delta\Delta G^\ddagger$
		min^{-1}	%		*kcal/mol*
Wild-type substrate (S11-mer)	GGGC**$G_5G_6G_7U_8C_9G_{10}G_{11}$**	0.34 ± 0.02	48.3 ± 0.9	1	
S10-mer	GGGC**GGGUCG**	0.022 ± 0.01	28.8 ± 4.3	0.063	−1.69
S9-mer	GGGC**GGGUC**	ND[a]	ND		
S8-mer	GGGC**GGGU**	ND	ND		
SG5A	GGGCAGGUCGG	0.009 ± 0.002	20.0 ± 2.4	0.026	−2.25
SG5C	GGGCCGGUCGG	0.047 ± 0.017	1.7 ± 0.2	0.138	−1.22
SG6A	GGGCGAGUCGG	0.026 ± 0.006	5.8 ± 0.5	0.076	−1.59
SG6U	GGGCGUGUCGG	0.071 ± 0.026	3.7 ± 0.3	0.209	−0.96
SG7A	GGGCGGAUCGG	ND	ND		
SG7U	GGGCGGUUCGG	ND	ND		
SU8C	GGGCGGGCCGG	ND	ND		
SU8G	GGGCGGGGCGG	ND	ND		
SC9A	GGGCGGGUAGG	0.016 ± 0.007	8.2 ± 3.0	0.047	−1.88
SC9U	GGGCGGGUUGG	0.031 ± 0.005	21.2 ± 1.0	0.091	−1.48
SG10U	GGGCGGGUCUG	0.016 ± 0.002	8.4 ± 0.5	0.047	−1.88
SG11U	GGGCGGGUCGU	0.011 ± 0.001	32.1 ± 2.5	0.032	−2.12

[a] ND, no detectable cleavage activity after a 3.5-h incubation period.

tions of δRzP1.1 for the gel shift analysis as described under "Materials and Methods." To ensure that the dissociation equilibrium was reached, we incubated the reaction mixtures at various intervals. We found that the equilibrium was reached within 5 min, and that a longer incubation of 28 h did not affect the measurement of K_d. Since SP1.1 can be cleaved under native gel electrophoresis conditions, we therefore used its analog which has a deoxyribose at position 4 (SdC4) to obtain the estimated K_d of the wild type substrate. This analog could not be cleaved by δRzP1.1 under the conditions used (2), and has been shown to be a competitive inhibitor of δRzP1.1 cleavage.[2] An example of a gel shift analysis carried out for the analog is shown in Fig. 4. In this particular analysis, trace amounts of SdC4 (<1 nM) were incubated with 11 concentrations of δRzP1.1 ranging from 5 to 600 nM. An autoradiogram of the resulting gel obtained by a Molecular Dynamics radioanalytic scanner is shown in Fig. 4, *panel A*. The bands of the bound SdC4 and the free SdC4 at each δRzP1.1 concentration were quantified, and the percentage of the bound SdC4 was plotted as shown in Fig. 4, *panel B*. The experimental data were fitted to a simple binding equation as described under "Materials and Methods" to obtain $K_d = 31.9 \pm 2.7$ nM. Similar experiments were performed for SG7A, SG7U, SU8C, and SU8G. The substrates in which A or U were substituted for G at position 7 were observed to have a lower affinity for δRzP1.1 than those of the substrates in which the U at position 8 is altered. The higher K_d values obtained for SG7A (320 ± 20 nM) and SG7U (220 ± 60 nM), as compared with those of the analog (31.9 ± 2.7 nM), SU8C (36.1 ± 2.5 nM), and SU8G (71.5 ± 3.2 nM) are summarized in Table III. We observed that the single mismatch introduced at position 7 disturbed the equilibrium of substrate-ribozyme complex formation to a greater extent than the mutation at position 8. The values of K_d were used in the determination of the free energy of substrate binding (Gibbs energy change, $\Delta G_{E\cdot S}$). The mismatch at position 7 interfered with the stabilization of the substrate-ribozyme complex, resulting in $\Delta\Delta G_{E\cdot S}$ between −0.43 and −1.4 $kcal^{-1}$ mol^{-1}.

[2] S. Mercure and J. P. Perreault, unpublished data.

DISCUSSION

δ ribozymes derived from the genome of HDV are of interest in the development of a gene regulation system in which the designed ribozymes would down-regulate the expression of a target gene. The facts that δ ribozymes are derived from HDV and that this pathogen naturally replicates in animal systems, suggest that this catalytic RNA could be used to control gene expression in human cells. Like other ribozymes, the designed ribozyme should specifically cleave its target substrates while leaving other cellular RNA molecules intact. We designed a *trans*-acting δ ribozyme harboring a recognition sequence similar to the HDV antigenomic δ self-cleaving motif so as to have a minimal system for the study of the specificity of the base pairing interaction between the δ ribozyme and its substrate.

Although a number of *trans*-acting δ ribozymes have been generated, they appear to have variable cleavage rate constants. The discrepancy of *cis*-acting δ ribozyme activities has been reviewed, and it was suggested that the variation of the cleavage activity, at least for *cis*-acting forms, may result from the nonribozyme flanking sequences used by each investigator (24). Our *trans*-acting δ ribozyme, δRzP1.1, exhibited an activity with a cleavage rate of 0.34 min^{-1}, or a $t_{1/2}$ of 2 min, under pseudo first-order conditions. These data are in good agreement with the observed rate constant (0.35 min^{-1}) of a *cis*-acting δ ribozyme derived from antigenomic HDV RNA (7). We found that the extent of cleavage is approximately 60%, regardless of the concentration of ribozyme used, suggesting possibilities that (i) a fraction of the substrate was bound to an inactive form of the δ ribozyme; (ii) substrate was bound to Cs of the 3′ of the ribozyme, instead of to the P1 region of the ribozyme, causing a misfold or a nonactive substrate-ribozyme complex; or (iii) a portion of the ribozyme might adopt another conformation following substrate binding. Based on the latter hypothesis, the alternative form of ribozyme-substrate complex could undergo cleavage at a very low rate. We first investigated whether or not the presence of the alternative form could be a result of an infidelity of the T7 RNA polymerase transcription. Two batches of purified T7 RNA polymerase were tested using various amounts of enzyme and incubation times (data not shown). We found that the transcripts produced by both

batches of purified T7 RNA polymerase at the different incubating times exhibited a similar cleavage pattern and extent, suggesting that it is the nature of ribozyme transcripts to adopt an alternative form in the reaction mixtures, as previously reported for the hairpin ribozyme (19). A possible occurrence of misplaced or misfold substrate-substrate complex was dismissed since there is no evidence of other formed complexes detected under nondenaturing gel electrophoresis and also by RNase mapping.[3] Finally, the possible occurrence of a slow cleaving form of δ ribozyme was assessed following cleavage reactions. We attempted to fit the experimental data using a multiphasic kinetic equation. Since we could not clearly describe the kinetics of our *trans*-acting δ ribozyme as biphasic or multiphasic reactions, we measured initial rates of cleavage for comparative purposes.

To summarize the cleavage reactions catalyzed by δRzP1.1 and δRzP1.2, free energy diagrams of the reaction coordinates were constructed (Fig. 5). The diagrams relate the two states in the cleavage reactions using kinetic parameters obtained under single turnover conditions. δRzP1.1 and δRzP1.2 differ in that they have two base pairs in the middle of the P1 stem interchanged. As expected, the free energies of substrate binding are virtually identical (-11 kcal^{-1} mol^{-1}). The base pair interchange in δRzP1.2 increased the value of $\Delta G‡$ by approximately 0.5 kcal^{-1} mol^{-1}. It is interesting to note that the free energy of the transition state was affected by the changes in the base pairing of the P1 stem. Although several kinetic parameters were greatly different from those reported here, similar findings were previously reported when two nucleotides (positions 7 and 8) of the substrate were interchanged and complemented by the δ ribozyme (12). Since the kinetics of δ cleavage reactions appear to be affected by the particular combination of base pairs, it is very likely that in addition to P1 base pairing a tertiary interaction might also participate in substrate recognition. In this scenario the substrate-ribozyme complex would undergo a conformational transition, following forma-

[3] D. Lafontaine and J. P. Perreault, unpublished data.

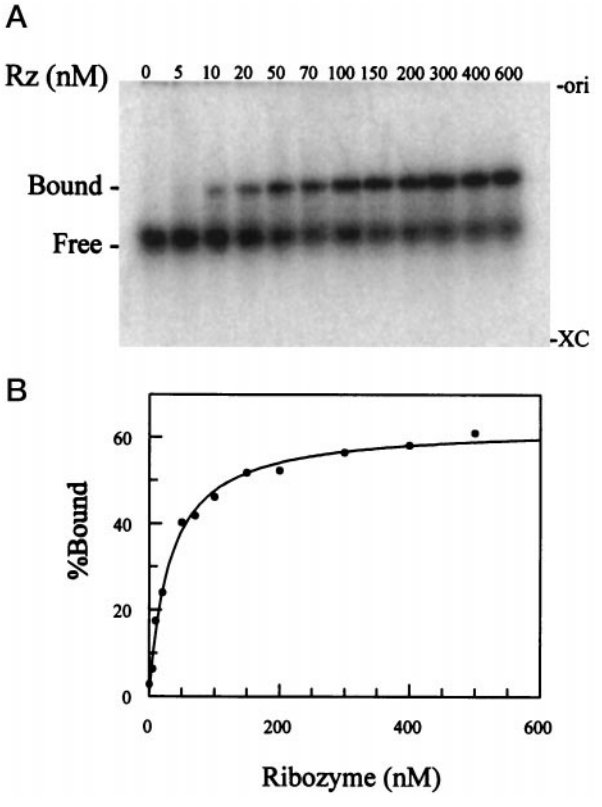

FIG. 4. **The measurement of equilibrium dissociation constant (K_d).** *Panel A*, an autoradiogram of a nondenaturing polyacrylamide gel. The gel fractionation separated labeled substrate (*Free*) from ribozyme-substrate complex (*Bound*) at various concentrations of δRzP1.1. The positions of the top of the gel (*ori*) and xylene cyanol (*XC*) are indicated. *Panel B*, the percentage of ribozyme-substrate complex (*Bound*) were quantified and plotted to fit a simple binding curve as described under "Material and Methods" with K_d = 31.9 ± 2.7 nM.

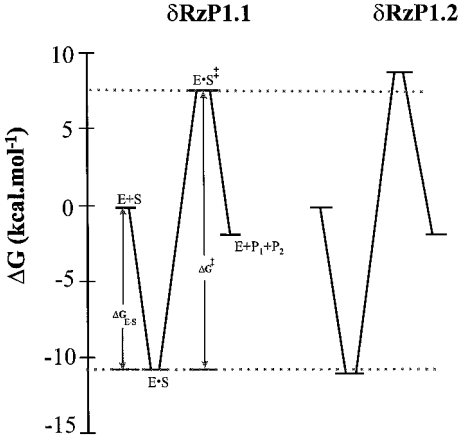

FIG. 5. **Free energy diagrams for cleavage reactions catalyzed by δRzP1.1 and δRzP1.2.** The cleavage reactions for δRzP1.1 (P1, CC**GA**CCU) and δRzP1.2 (P1, CC**CA**G**C**U) were carried out under similar conditions as described under "Materials and Methods." A standard state 1 M free substrate and ribozyme at 310.15 K (37 °C) is assumed to be the same for both δ ribozymes. Gibbs energy changes of the enzyme-substrate complex formation ($\Delta G_{E\cdot S}$) were calculated from an apparent K_m (K_m') using the equation, $\Delta G_{E\cdot S} = -RT \ln K_m'$. The K_m' is 17.9 nM for δRzP1.1 and 16.7 nM for δRzP1.2; the $\Delta G_{E\cdot S}$ is 10.9 kcal^{-1} mol^{-1} for δRzP1.1 and 11.0 kcal^{-1} mol^{-1} for δRzP1.2. Transition energy ($\Delta G‡$) is calculated from k_{cat} using the equation, $\Delta G‡ = -RT \ln k_{cat}\cdot h / k_B\cdot T$. The k_{cat} is 0.34 min^{-1} for δRzP1.1 and 0.13 min^{-1} for δRzP1.2; $\Delta G‡$ is 18.8 kcal^{-1} mol^{-1} for δRzP1.1 and 19.4 kcal^{-1} mol^{-1} for δRzP1.2. R, molar gas constant; h, Planck constant; k_B, Boltzman constant. *Dashed lines* indicate the values obtained for δRzP1.1.

TABLE III

Equilibrium dissociation constants of uncleavable single mismatched substrates as compared to the analog of the wild-type substrate

Bold letters and numbers in subscript represent the nucleotides and their positions in the analog recognized by ribozyme. The analog was designed to have a deoxyribonucleotide at position 4 of the wild-type substrate. K_d is equilibrium dissociation constant obtained from fitting the data to the equation % bound substrate = $[RZ]/K_d + [RZ]$, where $[RZ]$ is the concentration of ribozyme, and K_d is the equilibrium dissociation constant. $\Delta G_{E.S}$, the Gibbs energy change, is calculated using the equation $\Delta G_{E.S} = -RT \ln K_d$, where T = 310.15 K (37 °C) and R = 1.987 cal K$^{-1}\cdot$ mol^{-1}. $K_{rel} > 1$ indicates a destabilization effect of the given mismatched nucleotide. $\Delta\Delta G_{E.S}$ is the relative change of Gibbs energy obtained from either the equation $\Delta\Delta G_{E.S} = -RT \ln K_{rel}$, or from the difference between the values of $\Delta G_{E.S}$ of mismatched substrate and that of the analog.

Substrates	Sequence	K_d	$\Delta G_{E.S}$	K_{rel}	$\Delta\Delta G_{E.S}$
		nM	*kcal · mol^{-1}*		
Analog substrate (SdC4)	GGG**dC**$_4$G$_5$G$_6$G$_7$U$_8$C$_9$G$_{10}$G$_{11}$	31.9 ± 2.7	−10.6	1	
SG7A	GGGCGGAUCGG	320 ± 20	−9.2	10	−1.4
SG7U	GGGCGGUUCGG	220 ± 60	−9.4	7	−1.19
SU8C	GGGCGGGCCGG	36.1 ± 2.5	−10.6	1	0
SU8G	GGGCGGGGCGG	71.5 ± 3.2	−10.1	2	−0.43

tion of P1 stem, which involves tertiary interaction(s). These interactions might result in the positioning of the scissile bond in the catalytic center, a key step in the reaction pathway.

The substrate specificity of the δ ribozyme was studied using δRzP1.1. First, we found that the δ ribozyme can cleave a substrate having a minimum of 6 nucleotides adjacent to the cleavage site. This result is in an agreement with those previously reported for both the *cis*-acting form (5) and the *trans*-systems (11) that a minimum of 6 base pairing is required for cleavage. The k_{obs} of the 10-nt substrate is at least 10 times slower than that of SP1.1 (Table II). We also used shorter substrates generated by alkali hydrolysis as described by Perrotta and Been (11) to verify the cleavage reactions catalyzed by the two similar *trans*-acting δ ribozymes. Due to the slow cleavage rate, the detection of the disappearance of shorter substrates in the mixtures could not accurately be measured (data not shown).

Second, to estimate the contribution of base pairing interaction of the P1 stem to the cleavage reaction, a collection of single mismatched substrates was generated by introducing point mutations into the substrate sequence. Although there are a number of reports on the base pairing requirement of the P1 region (8, 10–12, 14), no extensive investigation has been performed on each individual nucleotide of either *cis*- or *trans*-acting δ ribozymes. The determination of ribozyme specificity against various substrates was first attempted by comparing the apparent second-order rate constant (k_{cat}/K_m') of each substrate to that of wild type substrate. We found that the ribozyme cleaved single mismatched substrates very slowly and gave a low percent cleavage (maximum of 2–20%) within the reaction time studied (3.5 h). As a consequence, the measurement of the apparent second-order rate constants as a function of ribozyme concentration yielded values with a high margin of error. We thus reported the cleavage activity of the ribozyme against various single mismatched substrates in terms of extent of cleavage and k_{obs}, which at a high ribozyme concentration reflects the k_{cat} of the cleavage reaction. In all cases, we observed the decrease in cleavage extent, which we suspected to be due mainly to the poor binding between the substrate and the ribozyme. The wobble base pair (G-U) at the cleavage site is required to maintain a high level of cleavage (10, 11). Mismatches at this position, which create either an A-U or a C-U pairing, decreased the cleavage activity in a manner analogous to that reported in another version of *trans*-acting δ ribozymes (10). It is interesting to note that the extent of cleavage decreases proportionally to the mismatches introduced into the 3′ and 5′ positions of the middle of the P1 stem. The simultaneous alteration of two nucleotides in the middle of the P1 stem was reported to give rise to an uncleavable substrate in both the *cis*- and *trans*-acting systems (11). However, in both cases the activity could be restored by the generation of a complementary ribozyme or a substrate.

The calculated free energy of transition-state stabilization ($\Delta\Delta G^{\ddagger}$) for each substrate listed in Table II varies between −0.9 and −2.25 $kcal^{-1}\ mol^{-1}$. Each position of base pairing between the substrate and the ribozyme appears to affect the reaction pathway differently, at least with regard to transition state complex formation. If we assume that mismatched substrates yield the same level of $\Delta G_{E\cdot S}$, various end points of cleavage for mismatched substrates could be resolved depending upon the height of the energy barrier level to be overcome in the transition state. To address these questions precisely, more experiments on the equilibrium binding constant and the internal equilibrium of the reactions are required. We have determined the calculated K_d of P1 duplex formation using the equation described by Serra and Turner (25) to be 28.5 nM. By using an analog, we have shown that the K_d of the wild type substrate to its ribozyme is 31.9 nM. It is very interesting to note that the mismatch introduced at position U8 of the substrate has little effect on substrate binding affinity. However, the change completely eliminated cleavage activity. The mismatch introduced at position G7 of the substrate affected both the binding and chemical steps since it not only lowered the binding affinity of the substrate for the ribozyme, but also destroyed the cleavage activity. These findings suggest that some base pairs of the P1 stem have dual roles, participating in the substrate binding and subsequent steps leading a chemical cleavage, as was observed for the base pair interactions between the hammerhead ribozyme and its substrates (26). To address these findings more precisely some preliminary experiments have been carried out using the metal-ion induced cleavage method to study the tertiary structure of δ ribozyme 3. The data obtained to date suggests that positions U8 and G7 are likely involved in the formation of an essential metal-ion binding site. The mismatches introduced at either of the two positions destroyed the formation of this metal-ion binding site, a process which has been found to be highly associated with cleavage activity.

We present here evidence that aside from the base pairing between the substrate and the ribozyme, tertiary interactions, especially ones involving the P1 stem, appear to dictate the reaction pathway of δ ribozyme. To fully comprehend how the cleavage reactions are governed, the elucidation of these tertiary interactions is essential.

Acknowledgments—We thank Dr. Stephane Mercure for the pδRzP1.1 construct.

REFERENCES

1. Lazinski, D. W., and Taylor, J. M. (1995) *RNA* (*New York*) **1,** 225–233
2. Perrotta, A. T., and Been, M. D. (1991) *Nature* **350,** 434–436
3. Wu, H. N., Lin, Y. J., Lin, F. P., Makino, S., Chang, M. F., and Lai, M. M. C. (1989) *Proc. Natl. Acad. Sci. U. S. A.* **86,** 1831–1835
4. Branch, A. D., and Robertson, H. D. (1991) *Proc. Natl. Acad. Sci. U. S. A.* **88,** 10163–10167
5. Kumar, P. K. R., Suh, Y. A., Taira, K., and Nishikawa, S. (1993) *FASEB J.* **7,** 124–129
6. Kawakami, J., Yada, K., Suh, Y. A., Kumar, P. K. R., Nishikawa, F., Maeda, H., Taira, K., Ohtsuka, E., and Nishikawa, S. (1996) *FEBS Lett.* **394,** 132–136
7. Wu, H. N., and Huang, Z. S. (1992) *Nucleic Acids Res.* **20,** 5937–5941
8. Wu, H. N., Wang, Y. J., Hung, C. F., Lee, H. J., and Lai, M. M. C. (1992) *J. Mol. Biol.* **223,** 233–245
9. Wu, H. N., Lee, J. Y., Huang, H. W., Huang, Y., and Hsueh, T. G. (1993) *Nucleic Acids Res.* **21,** 4193–4199
10. Nishikawa, F., Fauzi, H., and Nishikawa, S. (1997) *Nucleic Acids Res.* **25,** 1605–1610
11. Perrotta, A. T., and Been, M. D. (1992) *Biochemistry* **31,** 16–21
12. Been, M. D., Perrotta, A. T., and Rosenstein, S. (1992) *Biochemistry* **31,** 11843–11852
13. Makino, S., Chang, M. F., Shieh, C. K., Kamahora, T., Vannier, D. M., Govindarajan, S., and Lai, M. M. C. (1987) *Nature* **329,** 343–346
14. Fauzi, H., Kawakami, J., Nishikawa, F., and Nishikawa, S. (1997) *Nucleic Acids Res.* **25,** 3124–3130
15. Hertel, K. J., Herschlag, D., and Uhlenbeck, O. C. (1996) *EMBO J.* **15,** 3751–3757
16. Fedor, M. J., and Uhlenbeck, O. C. (1992) *Biochemistry* **31,** 12042–12054
17. Milligan, J. F., Groebe, D. R., Witherell, G. W., and Uhlenbeck, O. C. (1987) *Nucleic Acids Res.* **15,** 8783–8798
18. Been, M. D., and Perrotta, A. T. (1995) *RNA* (*New York*) **1,** 1061–1070
19. Esteban, J. A., Banerjee, A. R., and Burke, J. M. (1997) *J. Biol. Chem.* **272,** 13629–13639
20. Amiri, K. M., and Hagerman, P. J. (1996) *J. Mol. Biol.* **261,** 125–135
21. Traut, T. W. (1994) *Mol. Cell. Biochem.* **140,** 1–22
22. Chartrand, P., Usman, N., and Cedergren, R. (1997) *Biochemistry* **36,** 3145–3150
23. Fersht, A. R. (1988) *Biochemistry* **27,** 1577–1580
24. Been, M. D. (1994) *Trends Biochem. Sci.* **19,** 251–256
25. Serra, M. J., and Turner, D. H. (1995) *Methods Enzymol.* **259,** 242–261
26. Hertel, K. J., Peracchi, A., Uhlenbeck, O. C., and Herschlag, D. (1997) *Proc. Natl. Acad. Sci. U. S. A.* **94,** 8497–8502